可視化情報 Vol.22 Suppl. No.1 (2002年7月)

224 Wavelet Analysis of Turbulent Structures in Far Wake

Hui LI[O] (Kagoshima University), **Yu ZHOU** (The Hong Kong Polytechnic University)
Masahiro TAKEI (Nihon University), **Yoshifuru SAITO** (Hosei University)
Kiyoshi HORII (Shirayuri College)

Abstract

Initial condition effects in a self-preserving plane wake were investigated for two wake generators, i.e. a triangular cylinder and a screen of 50% solidity. Two orthogonal arrays of sixteen X-wires, eight in the (x, y)-plane, i.e. the plane of mean shear, and eight in the (x, z)-plane, which is parallel to both the cylinder axis and the streamwise direction, are used to simultaneously obtain velocity data in the experimental investigation. Measurements were made at x/h (x is the streamwise distance downstream of the cylinder and h is the height of the wake generator) = 330 for the triangular cylinder and 220 for the screen. A two-dimensional orthogonal wavelet transform is used to analyze the measured hot-wire data. This technique enables the turbulence structures of various scales to be separated and characterized. Discernible differences are observed between the two wake generators in the turbulence structures of large- down to intermediate-scales.

Keywords: Far Wake, Turbulence, Vortex, Wavelet Multi-resolution Analysis

1. Introduction

There has been accumulating experimental evidence that points to the persistence of initial conditions in the self-preserving region of a turbulent flow. Most of the evidence has been obtained in plane and axi-symmetric wake flows. The persistence of the effect of initial conditions in the self-preserving region seems to imply that the characteristics of the large-scale organised structures depended on initial conditions. Using a vorticity-based detection scheme, Zhou and Antonia [1] (1995) educed large-scale vortical structures in a self-preserving wake produced by different generators. Conditional sectional streamlines and contours of the shear stress indicated that the large-scale vortical structures in the self-preserving screen wake are more asymmetrical than in the self-preserving solid-body wakes. Accordingly, the contribution to the Reynolds shear stresses is appreciably larger in the screen wake than in the solid-body wakes. However, due to the limitation of their detection scheme, they could not provide any information on the dependence of organized structures other than the large-scale ones on the initial conditions. It is suspected that the organized structures of various scales all contribute to the dependence of a self-preserving wake on the initial conditions.

The present work aims to study the effect of initial conditions on the turbulent structures of various scales. Measurements were conducted in the far-wake generated by a triangular cylinder and a screen of 50% solidity, respectively. The wavelet multi-resolution analysis is used to decompose the measured velocity data into a number of wavelet components based on their central frequencies, which are representative of the turbulent structures of different scales. The flow structure of various scales is characterized and visualized by the sectional streamlines and vorticity contours of the wavelet components.

2. Wavelet Multi-resolution Analysis

The two-dimensional discrete vector wavelet transform of vector field $\vec{f}(x_1, x_2)$ is defined as

$$\overrightarrow{Wf}_{m;n_1,n_2} = \sum_i \sum_j \vec{f}(x_1^i, x_2^j) \Psi_{m;n_1,n_2}(x_1^i, x_2^j) \qquad (1)$$

where $\Psi_{m;n_1,n_2}(x_1, x_2)$ is a two-dimensional orthogonal wavelet basis and is defined as

$$\Psi_{m;n_1,n_2}(x_1, x_2) = 2^{-m} \psi(2^{-m} x_1 - n_1) \psi(2^{-m} x_2 - n_2) \qquad (2)$$

Here $\psi(x)$ is an one-dimensional orthogonal wavelet basis.

The reconstruction of the original vector field can be achieved by using

$$\vec{f}(x_1,x_2)=\sum_{m}\sum_{n_1}\sum_{n_2}\overrightarrow{Wf}_{m;n_1,n_2}\Psi_{m;n_1,n_2}(x_1,x_2) \quad (3)$$

Since the discrete wavelet transform is a linear transform, the wavelet multi-resolution analysis is used to completely decompose a non-linear problem into the superposition of a limited number of grouped frequency components (from low frequency to high frequency). Hence, Eq. (3) can be written in the following equivalent form:

$$\vec{f}(x_1,x_2)=\overrightarrow{fw}_1+\overrightarrow{fw}_2+\cdots+\overrightarrow{fw}_k \quad (4)$$

where

$$\overrightarrow{fw}_i=\sum_{n_1}\sum_{n_2}\overrightarrow{Wf}_{i;n_1,n_2}\Psi_{i;n_1,n_2}(x_1,x_2) \quad (5)$$

On the right side of Eq. (5), the first term $\overrightarrow{fw}_1$ and the last term $\overrightarrow{fw}_k$, represent the components at level *1* (the lowest frequency) and level *k* (the highest frequency).

The procedure of the wavelet multi-resolution analysis can also be summarized in two steps:

(1) Wavelet coefficients are computed based on the discrete wavelet transform of Eq. (1).

(2) Inverse vector wavelet transform of Eq. (3) is applied to wavelet coefficients at each wavelet level, and components are obtained at each level or scale.

It is evident that a sum of all frequency components can reconstruct the original vector function. Therefore, the wavelet multi-resolution analysis may process fewer data by selecting the relevant details that are necessary to perform an extraction of the multi-scale structures, and decompose the vector data in both Fourier and physical spaces. In this study, we use the Daubechies family with index N=20 as the orthogonal wavelet basis.

This wavelet multi-resolution technique was discussed in detail by Li and Zhou [2] and therefore not repeated here.

3. Experimental Setup

Experiments were carried out in an open return low turbulence wind tunnel with a 2.4 m long working section (0.35 m x 0.35 m). The bottom wall was tilted to achieve a zero streamwise pressure gradient. A triangular cylinder (h = 6.35 mm) and a screen (h = 8.0) of 50% solidity were used to generate the wake, respectively; each was installed in the mid-plane and spanned the full width of the working section, 0.20 m from the exit plane of the contraction. The two generators corresponded to a blockage of 1.8% and 1.2%, respectively. Measurements were made at U_0 = 6.7 m/s, resulting in different Reynolds number for the two generators.

Using two orthogonal arrays, each comprising eight X-wires (Figure 1), velocity fluctuations *u, v* in the (*x, y*)-plane and *u, w* in the (*x, z*)-plane were obtained simultaneously. The nominal spacing between X-wires in both planes was about 5 mm except for a relatively large gap (= 9.1 mm) between the fourth and fifth X-wires in the (x, z)-plane. The arrays were attached to separate traversing mechanisms and could be moved independently of each other. The eight X-wires in the (*x, y*)-plane were fixed with the second X-wire (from the bottom) positioned approximately on the centerline; the eight X-wires in the (*x, z*)-plane were located at about 10 mm above the centerline.

Signals from the circuits were offset, amplified and then digitized at a sampling frequency of 3.5 kHz per channel (the cut-off frequency was 1600Hz). Data acquisition by the two computers was synchronized using a common external trigger pulse. The duration of each record was about 38 sec.

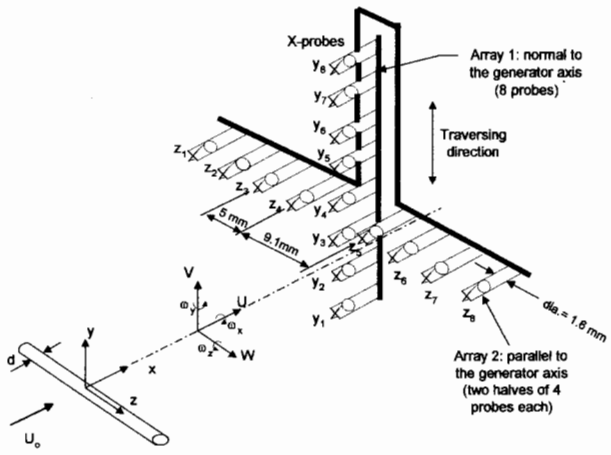

Fig.1 Experimental arrangement

4. Wavelet Decomposition Method

An instantaneous velocity vector $\vec{U}(x,y,z,t)$ can be written as the sum of a time-averaging component $\overline{\vec{U}}(x,y,z)$ and a fluctuating component $\vec{u}(x,y,z,t)$, viz.

$$\vec{U}(x,y,z,t)=\overline{\vec{U}}(x,y,z)+\vec{u}(x,y,z,t) \quad (6)$$

In order to gain insight into the turbulent structures of various scales, the vector wavelet multi-resolution technique is used to decompose the velocity fluctuation component $\vec{u}(x,y,z,t)$ into a number of wavelet components based on wavelet levels, which correspond to the central frequencies or scales and are directly linked to the turbulent structure scales. Each wavelet component represents the turbulent structures of a certain range of frequencies (i.e. a non-zero frequency band) so that the information of any scales contained in the original data will not be lost because of a limited number of wavelet components. Since a time sequence of 65536 points at each of X-wire position are analyzed in this study, the thirteen wavelet components are obtained presently and $\vec{u}(x,y,z,t)$ may be given by

$$\vec{u}(x,y,z,t)=\sum_{j=1}^{13}\vec{u}_j(x,y,z,t) \qquad (7)$$

where $\vec{u}_j(x,y,z,t)$ is the wavelet component of $\vec{u}(x,y,z,t)$ at the *jth* wavelet level. Accordingly, the instantaneous velocity in the *jth* wavelet component is given by

$$\vec{U}_j(x,y,z,t)=\vec{\overline{U}}(x,y,z)+\vec{u}_j(x,y,z,t) \qquad (8)$$

The wavelet components of spanwise vorticity may be computed based on velocity data at each of the wavelet level using the central difference approximation. Thus, the eight X-wires in the (x, y)-plane may produce the thirteen-wavelet components of spanwise vorticity at each of the seven midpoints between adjacent X-wires. The wavelet component of spanwise vorticity at the *jth* wavelet level may be approximated by

$$\omega_{zj}=\frac{\partial V_j}{\partial x}-\frac{\partial U_j}{\partial y}=\frac{\partial v_j}{\partial x}-\frac{\partial(\overline{U}+u_j)}{\partial y}\approx\frac{\Delta v_j}{\Delta x}-\frac{\Delta(\overline{U}+u_j)}{\Delta y} \qquad (9)$$

where $U_j=\overline{U}+u_j$ and $V_j\approx v_j$ ($\overline{V}\approx 0$). In Eq. (9), Δy (≈ 5.0 mm) is spacing between two X-wires in the (x, y)-plane; $\Delta x = -\overline{U}_c\,\Delta t = -\overline{U}_c/f_s$. For simplicity, the average vortex convection velocity $\overline{U}_c = 0.95U_0$ on the vortex path is used to calculate Δx. Vorticity contours and rms values thus obtained showed no appreciable difference from those obtained using the local mean velocity.

5. Results and Discussion

The power spectrum of the v-signal exhibits a prominent peak around the frequency f_0, which is 60 Hz and 90 Hz in the triangular cylinder and screen wakes, respectively. The central frequency f_0 represents the average frequency of the large-scale vortical structures.

In order to better visualize instantaneous turbulent structures of various scales, sectional streamlines were constructed for each wavelet component of velocity as well as for measured velocities. Figure 2 shows the instantaneous sectional streamlines overlapping on the vorticity contours normalised vorticity $\omega_z L/U_0$ in the

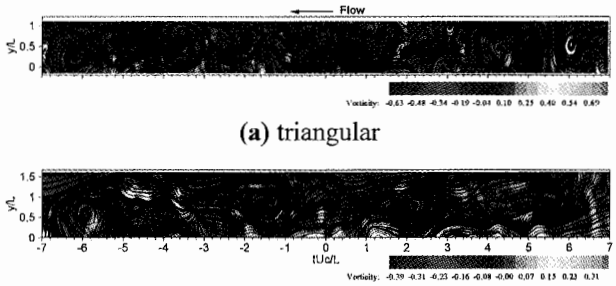

(a) triangular

(b) screen

Fig.2 Measured sectional streamlines and vorticity contours in the (x, y)-plane

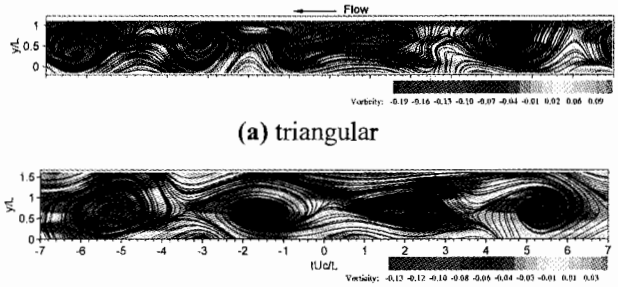

(a) triangular

(b) screen

Fig.3 Sectional streamlines and vorticity contours of the wavelet component at f_0

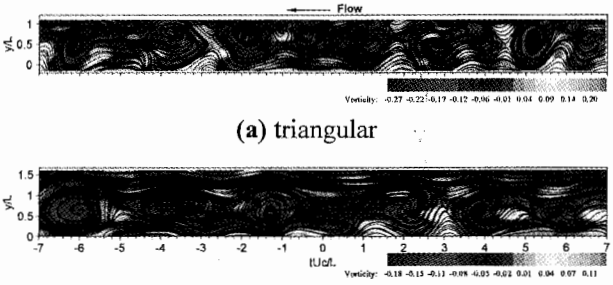

(a) triangular

(b) screen

Fig.4 Sectional streamlines and vorticity contours of the wavelet component at $2f_0$

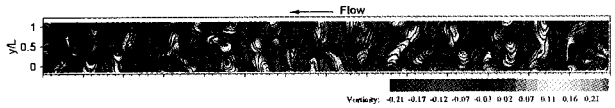

(a) triangular

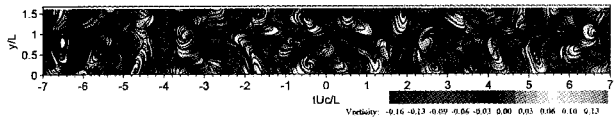

(b) screen

Fig.6 Sectional streamlines and vorticity contours of the wavelet component at $4f_0$

triangular cylinder and screen wakes in the (x, y)-plane for measured data. The vertical axis is the spatial coordinate plotted in half width units. The horizontal axis is the temporal coordinate plotted also in half width units after converting the time displacements into spatial ones by using the average convection velocity of vortical structures. The timescale is increasing from left to right in such a way that the flow is observed moving from right to left. The false colors have been assigned to the scalar values of vorticity; the highest and lowest vorticities are respectively displayed as red and blue. The positive and negative vorticities denote clockwise and counterclockwise vortices, respectively. It is suggested that the triangular cylinder and screen wakes have different geometrical characteristics of the vortex structure, e.g., shape, size, and spacing of the vortices. The maximum strength of spanwise vorticity in the triangular cylinder wake is larger than that in the screen wake. It is difficult to identify the dependence of various scale structures on the initial conditions in the measured streamlines for both the triangular cylinder and screen wakes.

Figures 3-6 present sectional streamlines and vorticity contours of different scales in the (x, y)-plane for the triangular cylinder and screen wakes, calculated from the wavelet components of velocity at the central frequencies of f_0, $2f_0$ and $4f_0$. As discussed above, the component of the central frequency f_0 represents the large-scale vortical structures. The sectional streamlines and vorticity contours of the component display a flow pattern similar to the conditional averaged results[1], thus providing a validation of the present used data analysis technique. In Fig.3, four instantaneous vortical structures of the central frequencies f_0 are easily extracted in both the triangular and screen wake. These structures correspond quite well to the large-scale structures in Fig.2. The size of the vortical structures from f_0 to $4f_0$ in the screen wake appears to be considerably larger than in the triangular cylinder wake. However, the maximum strength of spanwise vorticity at each scale in the triangular cylinder wake is larger than that in the screen wake. It indicates that the organized structures of various scales depended on the initial conditions in the self-preserving region.

6. Conclusions

The self-preserving wake generated by a triangular cylinder and a screen, respectively, has been investigated with a view to provide information on the possible effect of initial conditions on turbulence structures of various scales. It is confirmed that the organized structures of various scales depended on the initial conditions in the self-preserving region. Furthermore, the wavelet components up to four times the central frequency of turbulent structures also display discernible difference between the two wakes, indicating an effect of initial conditions on intermediate-scale structures as well as large-scale ones.

References

(1) Zhou, Y. & Antonia, R. A., "Memory Effects in Turbulent Plane Wakes", *Experiments in Fluids*, Vol.19 (1995), pp.112-120.

(2) Hui LI, Y. Zhou, M. Takei, Y. Saito and K. Horii, "Visualization of Turbulent Structure From the Wavelet Analysis of Multipoint Hot-Wire Data", *Proceedings of the 3rd Pacific Symposium on Flow Visualization and Image Processing*, USA (2001), No.F3302, pp.1-11.